

Edyta OSUCH-SŁOMKA*

ABRASIVE WEAR MECHANISMS OF ANTIWEAR COATINGS IN BALL-CRATERING TESTS

MECHANIZMY ZUŻYWANIA ŚCIERNEGO POWŁOK PRZECIWZUŻYCIOWYCH W METODZIE BALL-CRATERING

Key-words:

antiwear coatings, abrasive wear mechanisms, ball-cratering method

Słowa kluczowe:

powłoki przeciwzużyciowe, mechanizmy zużycia ściernego, metoda ball-cratering

Abstract

The article is a continuation of research on the mechanisms of wear on PVD coatings observed after tests had been performed with the use of the ball-cratering method evaluating the wear. The work conditions of friction point in which tribological tests had been performed were calculated based on the optimization experiments described in independent studies [L. 1–2]. The aim of the article is to analyse the boundary surface coating–substrate resulting from abrasive wear. The observed area is located on the border of the trace of wear in the shape of a crater, at the point of the exit of the ball from the

* Institute for Sustainable Technologies – National Research Institute, 26-600 Radom, ul. Pułaskiego 6/10, Poland, tel. (048) 36-442-41, fax (048)63-447-65, e-mail: edyta.slomka@itee.radom.pl.

trace in accordance with the direction of the selection of the coating. The tested surface was observed with the use of microscopic techniques: scanning electron microscope (SEM) and interferometric microscope (WLI).

The authors attempted to present the repetitive nature of the mechanism of the wear of thin PVD coatings with the use of the ball-cratering method, including its influences on receiving repeated traces of wear, which, in turn, has an influence on the determination of a reproducible value of the wear rate Kc , which is the factor determining the resistance of the tested coating to abrasive wear.

INTRODUCTION

Abrasion is the most common type of wear. In most cases, it occurs in the relative movement of the associated components of machine parts. The fundamental processes occurring on the abrasive wear are ploughing and micro cutting. The difference between these processes is the shape of grain or cutting surface irregularities that usually occur at the same time, which affects the intensity of abrasive wear. According to the Polish Standard PN-91 / M-04301 [L. 3], abrasive wear is the wear of friction surfaces of the bodies as a result of elementary mechanical wear processes, such as microcutting, drawing, ploughing, and grain pull-out. The intensity of wear depends on many factors: the abrasive properties (hardness, size, and shape of the grain), the properties of the abrasive material (hardness), and the work conditions (load, speed, distance) [L. 4].

MATERIALS AND METHODS

The tests were conducted on a test bench T-20¹ with the use of the ball-cratering method. The ball-cratering method is used to test the wear resistance of coatings and construction materials. It is a method that requires the selection of the values of parameters (load, speed, and at least four sliding distances) that will be correct for the tested type of coating. As required by its authors [L. 1–2], the pre-condition for the effectiveness of the methods are "round" craters of traces of wear, where the relative error of measured diameters should not exceed 10% [L. 7].

With the optimum work parameters of friction node, abrasive wear tests were performed on chosen anti-wear PVD coatings, then the factor of resistance to abrasive wear was calculated based on which the evaluation of their resistance to abrasive wear was conducted [L. 1–2].

¹ <http://www.itee.radom.pl/oferta/aparatura.htm>.

The measurement of the diameters of the traces of wear in the shape of craters was made with the use of a Nikon optical measuring microscope MM 40. The observed area is on the border of the trace of wear, which is the crater at the exit point of the ball in accordance with the direction of the selection of the coating (**Fig. 1**).

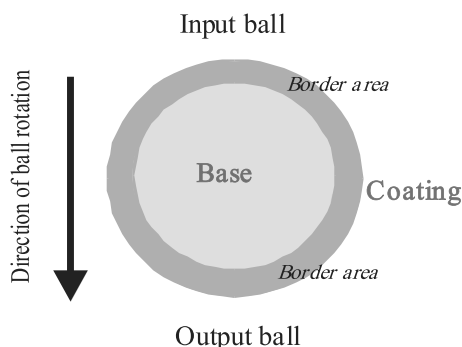


Fig. 1. Wear scar with direction of ball rotation

Rys. 1. Ślad zużycia z opisanym kierunkiem rotacji kuli

The test involved samples in the form of a disc of a diameter of 25.4 mm, 10 mm thick, made of WCLV steel (X40CrMoV5-1 DIN, ASTM H13) with a hardness of 55 HRC. The PVD coating, having the properties shown in **Table 1**, was deposited onto the discs. The parameters of the nitriding process are shown in **Table 2**.

Table 1. Properties of the PVD coatings

Tabela 1. Właściwości osadzonej powłoki PVD

Coating deposition	Thickness	Roughness	Hardness	Young's modulus	Cohesion	Adhesion
	g [μm]	R_a [μm]	HV	E [GPa]	L_{c2} [N]	L_{c3} [N]
CrN	3.2	0.37	1720±146	300 ±35	32	64
duplex/ CrN	3.5	0.35	1860±250	300 ±21	104	156
AlTiN	2.2	0.14	3200±100	440±10	30	60
duplex/AlTiN	2.0	0.15	3100±100	440±15	30	60
AlCrN	1.8	0.19	2400±350	350±66	14	70
(TiN/AlCrN)x5	2.25 0.16 – TiN 0.29 – AlCrN	0.20	2400±160	305±12	26	55

Table 2. Parameters of the ion nitriding process

Tabela 2. Parametry procesu azotowania

Process	Pressure	Atmosphere	Potential	U_{BIAS}	Temperature	Time	Thickness of the nitrided layer
	P[mbar]	[%]	$p(N^+/H^+)$	U[V]	T[°C]	t[min.]	[μm]
Ion nitriding	4.3	N ₂ 20% H ₂ 80%	2.0	-600	520	420	70

Measurements of the roughness of the surface of deposited coatings were performed with the use of a Taylor Hobson profilograph. The coatings were also tested for adhesion by the scratching method with the use of type C Rockwell indenter – REVETEST CSEM Tester, using a progressively increasing load up to 100N with a constant rate of increase in load of 10 N/mm. The values of the forces that cause specific mechanisms for the destruction of the coating were determined by microscopic observation of the damage to the coating within the area of scratches. Measurements of hardness and Young's modulus were performed with the use of Nano-Hardness Tester CSEM equipped with a Berkovich indenter, using a recess indentation not exceeding 10% of the thickness of the coating.

A counter sample in tribological tests was a spherical ball bearing with a diameter of 25.4 mm, made of steel 100Cr6 (ASTM 52100 from the company Dejay Distribution Limited, UK) of 58.6 HRC hardness and surface roughness of $R_a = 0.177 \mu\text{m}$. The abrasive was SiC powder (SiC/F1200-C6 produced by Abrasive Washington Mills, Manchester, United Kingdom) with particles of an average size not exceeding $4.0 \mu\text{m}$ and a hardness of 3000 HV [L. 5–6]. In the tests, a 20% SiC solution with distilled water was used.

Experimental results and discussions

Table 3 shows the signs of wear obtained for thin antiwear coatings after tribological tests conducted with the use of the ball-cratering method. Traces have a circular shape and a comparable thickness of the ring. The tests were performed at four lengths of sliding distance, which was necessary for determining the final parameter values of tests, namely, the abrasive wear coefficient (K_c) of the tested PVD coatings [L. 1].

As a result of microscopic examinations performed on the SEM SU-70 Hitachi microscope (**Table 4, 5**) and the interferometric Taylor Hobson microscope (**Table 6**), the areas of wear-through on the border of the system (coating–substrate) were presented. These areas were created as a result of the

Table 3. Optical images of the crater after tribological tests

Tabela 3. Obrazy kraterów otrzymane po badaniach zużyciowych

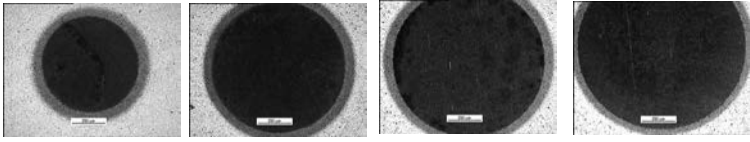
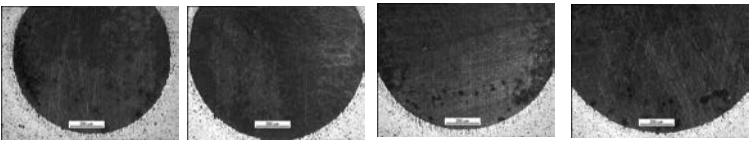
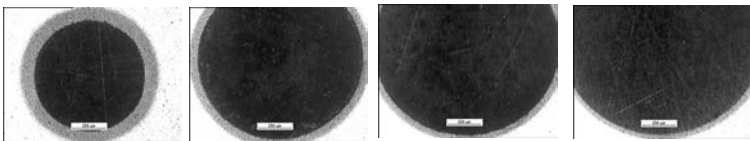
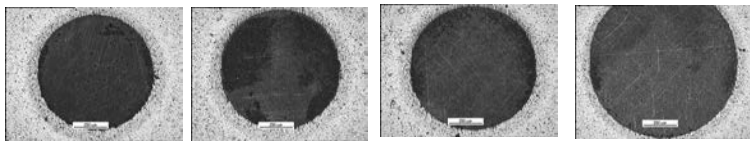
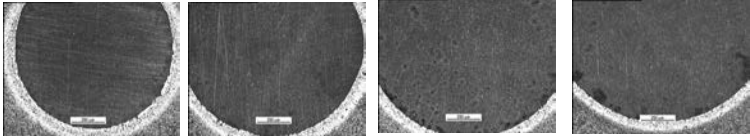
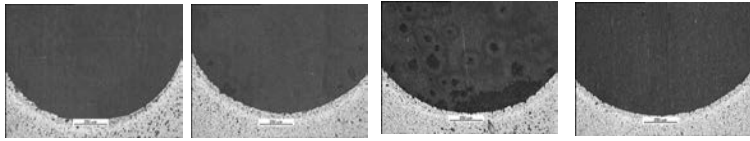
PVD coating	Work parameters
CrN	Load: 0.2 [N], speed of rotation: 150 [rpm] Four sliding distances: 12 [m], 40 [m], 68 [m], 96 [m]
	
AlTiN	Load: 0.6 [N], speed of rotation: 80 [rpm] Four sliding distances: 54[m], 72 [m], 90 [m], 108 [m]
	
duplex/CrN	Load: 0.4 [N], speed of rotation: 150 [rpm] Four sliding distances: 12 [m], 40 [m], 68 [m], 96 [m]
	
duplex/AlTiN	Load: 0.2 [N], speed of rotation: 150 [rpm] Four sliding distances: 60 [m], 73 [m], 87 [m], 100 [m]
	
AlCrN	Load: 0.6 [N], speed of rotation: 80 [rpm] Four sliding distances: 60 [m], 80 [m], 100 [m], 120 [m]
	
(TiN/AlCrN) x5	Load: 0.2 [N], speed of rotation: 80 [rpm] Four sliding distances: 75 [m], 105 [m], 135 [m], 165 [m]
	

Table 4. SEM images for border area between the coating and the substrate (magnification 1000x)

Tabela 4. Zdjęcia SEM z obszaru granicznego między powłoką a podłożem (powiększenie 1000x)

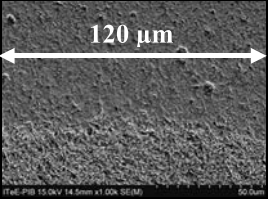
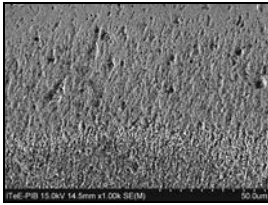
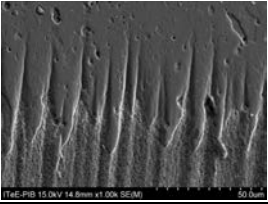
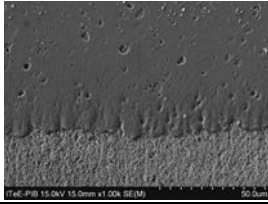
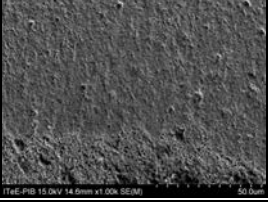
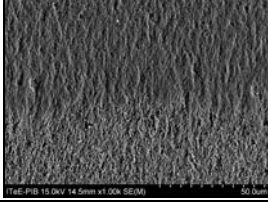
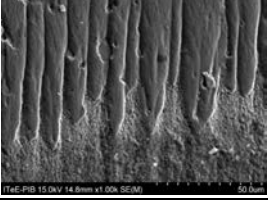
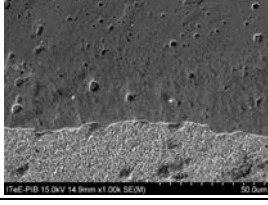
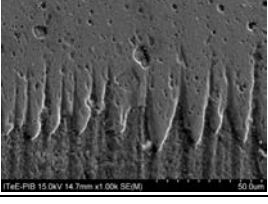
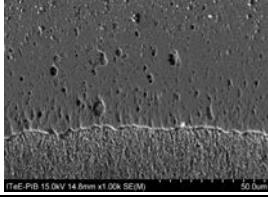
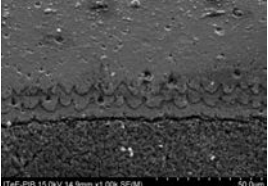
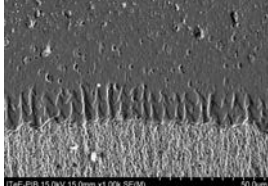
PVD coating	Distance 1	Distance 4
CrN		
AlTiN		
Duplex/CrN		
Duplex/AlTiN		
AlCrN		
(TiN/AlCrN)x5		

Table 5. SEM images for border area between the coating and the substrate (magnification 4000x)

Tabela 5. Zdjęcia SEM z obszaru granicznego między powłoką a podłożem (powiększenie 4000x)

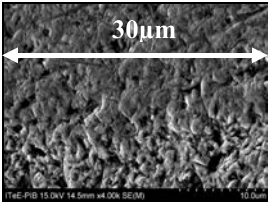
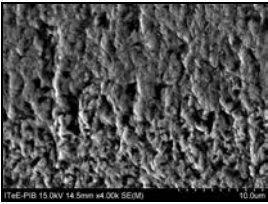
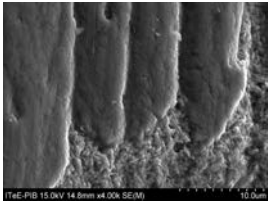
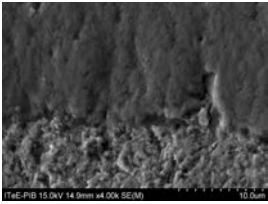
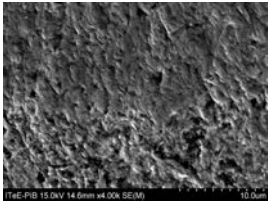
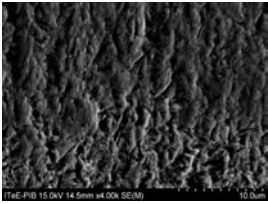
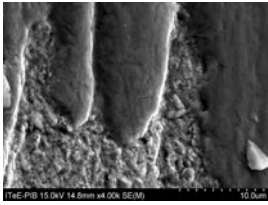
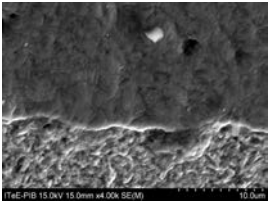
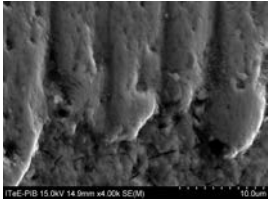
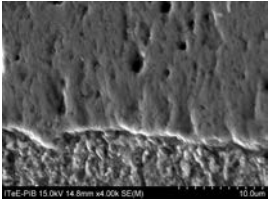
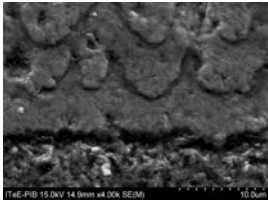
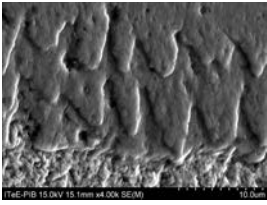
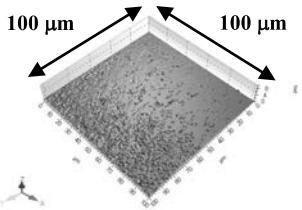
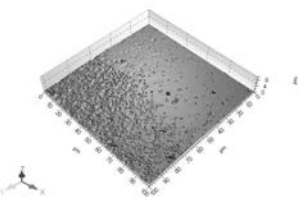
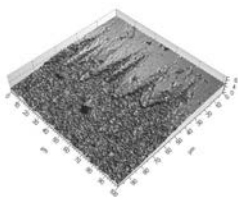
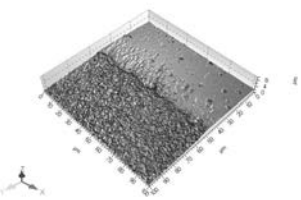
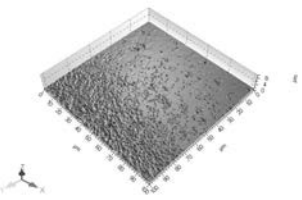
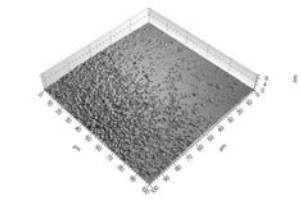
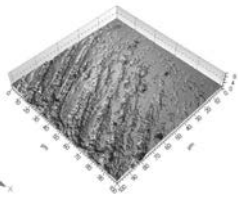
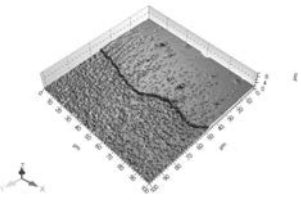
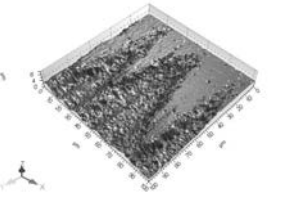
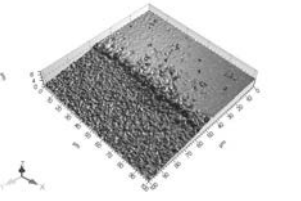
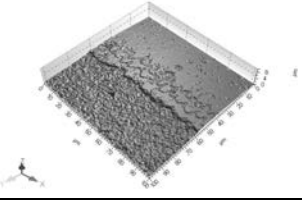
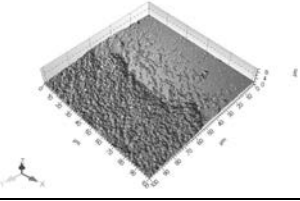
PVD coating	Distance 1	Distance 4
CrN		
AlTiN		
Duplex/CrN		
Duplex/AlTiN		
AlCrN		
(TiN/AlCrN)x5		

Table 6. Interferometry images for border area between the coating and the substrate

Tabela 6. Zdjęcia z obszaru granicznego między powłoką a podłożem wykonane przy użyciu mikroskopu interferometrycznego

PVD coating	Distance 1	Distance 4
CrN		
AlTiN		
Duplex/CrN		
Duplex/AlTiN		
AlCrN		
(TiN/AlCrN)x5		

abrasion of the coating after the performance of wear tests with the use of the ball-cratering method, in accordance with the direction of the selection of the coating by the ball (**Fig. 1**). The selected area of exit of the ball is characterized by the identical wear as in the border area of the entrance of the ball. The aim of the observation was to present the wear mechanisms occurring in the analysed border area [**L. 6–8**]. The surfaces of the crater on the border of the worn-through area on the coating were compared with the use of the determined optimum values of the operating parameters [**L. 1–2**]. After the performance of tribological tests, a significant difference in the wearing-away of the deposited PVD coatings was observed. In each tribological analysis, the forms of wear were reproducible. For coatings CrN and duplex/CrN, turning forms of wear were observed (three-body abrasive wear). For the coatings AlTiN, duplex/AlTiN, AlCrN, and (TiN/AlCrN) x5, ploughing (two-body abrasive wear) was predominate. The diverse nature of abrasive wear, according to the authors, is conditioned by the diverse hardness of the tested coatings with respect to the abrasive used, which has a hardness estimated at 3000HV. For example, the CrN coating is a relatively soft layer having a hardness of 1700-1800HV, compared to the hardness of the AlTiN coating of 3200-3300HV (**Tab. 1**). All analysed PVD coatings of hardness above 2000 HV are characterized by the occurrence of a ploughing mechanism on the worn boundary surface. Another cause for observing various forms of abrasive wear, according to the authors, is conditioned by the load values used at the friction point. The CrN coating load was 0.2 N, and for the AlTiN or AlCrN coating, it was 0.6 N. The low value of the load used for the CrN coating allowed the abrasive SiC grains to move freely in between the two bodies which led to the creation of the turning form of wear (three-body abrasive wear). With three times higher load, the distance between the two bodies decreased, thereby preventing the free movement of abrasive particles in the friction point, which initiated the creation of ploughing forms of wear (two-body abrasive wear).

With the increase in length of sliding distance and decreased unit pressure (**Fig. 2**) interacting in the friction point, the dominant forms of wear were turning and ploughing [**L. 9–10**].

Analysing the unit pressure curves (**Fig. 2**), a decline in pressure values in relation to the distance function was observed. The longer the distance, the lower the pressure values, because the surface of wear is greater. Due to the decreasing pressure values in the border area of the trace of wear of the coating–substrate, definitely shorter and shallower grooves in each case of analysed coating surface were observed after passing the fourth distance.

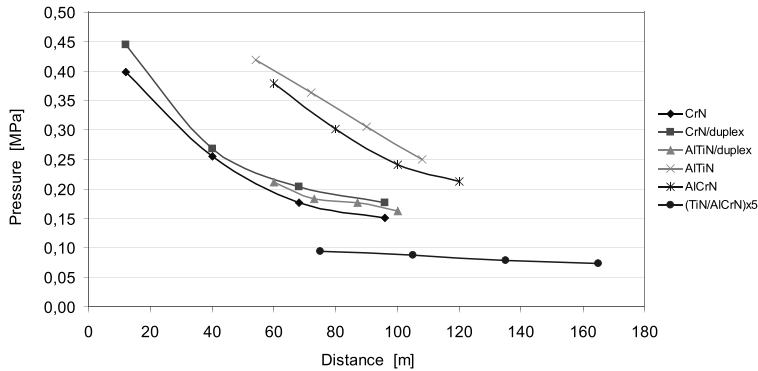


Fig. 2. The pressure on the surface of trace of wear
 Rys. 2. Naciski jednostkowe na powierzchni śladów

The values of the pressure were obtained from equations (1–3):

$$p = \frac{F}{A} \left[\frac{N}{mm^2} \right], \tag{1}$$

where $A = \pi r^2 = \frac{\pi D^2}{4} \left[mm^2 \right]$ (2)

$$p = \frac{4F}{\pi D^2} \left[\frac{N}{mm^2} = MPa \right] \tag{3}$$

Where p – pressure, F – normal force, A – diameter of wear scar.

While analysing the values of coefficients of the Kc coating wear, comparing the results of all of the tested coatings, it was found that the coating most resistant to wear is the AlTiN coating, both on an nitrided substrate and after heat treatment. The coefficient Kc for the AlTiN coating in comparison to the Kc coefficient for the CrN coating deposited on the substrate after the nitriding process and heat treatment is ten times lower. The detailed tests results are presented in paper [L. 1].

CONCLUSIONS

Having analysed the results of the tests, the following conclusions may be drawn:

- The ball-cratering method provided, throughout the wear test, a repetitive wear mechanism for thin PVD coatings.
- The nature of the observed forms of wear is associated with differing hardness values of the tested PVD coatings.

- Extending the sliding distance (hard AlCrN, AlTiN coatings) resulted in a change in unit pressure in the friction point and an increase in the turning of abrasive, which led to smoothing out of the grooves on the surface.
- Tests have shown that the both forms of wear (turning and ploughing) exist side by side. Changing the unit pressure and hardness of the coatings showed that the predominant form of wear is ploughing. Only on the CrN and CrN/duplex coating was the turning form of wear observed.

REFERENCES

1. Osuch-Słomka E, Ruta R and Słomka Zb. The use of a modern method of designing experiments in ball-cratering abrasive wear testing. Proc IMechE, Part J: J Engineering Tribology 2013; 227 (10): 1177–1187.
2. Osuch-Słomka, E. Proposed method for determining the values of tests for the ball-cratering method. Tribologia, 2011, 240, 161–171.
3. Norma PN-91/M-04301 Tribologia. Terminologia podstawowa.
4. Zwierzycki W. (pod red.) Selected problems of wear of the materials in sliding machines pairs. PWN Warszawa–Poznań 1990, *in Polish*.
5. Shipway P.H., Hogg J.J.: Wear of bulk ceramics in micro-scale abrasion – The role of abrasive shape and hardness and its relevance to testing of ceramic coatings. Wear 263/2007, p. 887–895.
6. Gee M.G, Gant A., Hutchings I., et al.: Progress towards standardisation of ball-cratering. Wear 255/2003, p. 1–13.
7. EN 1071-6:2007. Advanced technical ceramics – Methods of test for ceramic coatings- Part 6: Determination of the abrasion resistance of coatings by a micro-abrasion wear test.
8. Çalişkan H., et al. Micro-abrasion wear testing of multilayer nanocomposite TiAlSiN/TiSiN/TiAlN hard coatings deposited on the AISI H11 steel. Materials and technology, 2013, 47(5), 563–568, ISSN 1580-2949.
9. Cozza C.R.: Effect of sliding distance on abrasive wear modes transition. Journal of Materials Research and Technology, 2015, 4(2):144–150.
10. Cozza C.R., Schön G.C.: Evidence of superposition between grooving abrasion and rolling abrasion. Tribology Transactions, 04/2015. DOI: 10.1080/10402004.2015.1024907.

Streszczenie

Artykuł jest kontynuacją prezentacji wyników badań dotyczących analizy mechanizmów zużywania cienkich powłok PVD zaobserwowanych po badaniach zużyciowych metodą ball-cratering. Warunki pracy węzła tarcia, dla których wykonano badania tribologiczne opracowano na podstawie eksperymentów optymalizacyjnych opisanych w pracach własnych [L. 1–2]. Celem artykułu jest analiza powierzchni granicznej powłoka–podłoże

powstalej w wyniku zużycia ściernego. Obserwowany obszar znajduje się na granicy śladu zużycia w kształcie krateru, w miejscu wyjścia kuli ze śladu zgodnie z kierunkiem wybierania powłoki. Badaną powierzchnię obserwowano z zastosowaniem technik mikroskopowych: elektronowego mikroskopu skaningowego (SEM) i mikroskopu interferometrycznego (WLI). Założeniem autora było uzyskanie powtarzalnego charakteru mechanizmu zużywania cienkich powłok PVD metodą ball-cratering. Wpływa on na otrzymywanie powtarzalnych śladów zużycia, co z kolei ma wpływ na wyznaczenie powtarzalnej wartości współczynnika szybkości zużywania K_c , współczynnika określającego odporność badanej powłoki na zużycie ścierne.

Celem obserwacji było zaprezentowanie mechanizmów zużywania występujących na analizowanym obszarze granicznym [L. 6, 8]. Porównano powierzchnie krateru na granicy przetarcia powłoki przy wyznaczonych optymalnych wartościach parametrów pracy [L. 1–2]. Po przeprowadzonych biegach tribologicznych zaobserwowano znaczącą różnicę w ścieraniu osadzonych powłok PVD. W każdym z przeprowadzonych biegów tribologicznych formy zużycia były powtarzalne. Dla powłok: CrN, CrN/duplex zaobserwowano formę zużycia przez toczenie, natomiast dla powłok: AlTiN, AlTiN/duplex, AlCrN i (TiN/AlCrN) \times 5, *two-body abrasive wear* – przez bruzdowanie. Zróżnicowany charakter zużycia ściernego uwarunkowany jest zróżnicowaną twardością badanych powłok względem użytego ścierniwa, którego twardość wynosi 3000 HV. Dla przykładu powłoka CrN jest stosunkowo miękką powłoką o twardości 1700–1800 HV, w porównaniu z powłoką AlTiN o twardości 3200–3300 HV. Wszystkie analizowane powłoki PVD o twardości powyżej 2000 HV charakteryzują się występowaniem mechanizmu bruzdowania. Zróżnicowanie form zużycia ściernego spowodowane jest również wartościami zastosowanych obciążeń węzła tarcia. Dla powłoki CrN obciążenie wynosiło 0,2N, natomiast dla powłoki AlTiN czy AlCrN 0,6N. Niska wartość zastosowanego obciążenia dla powłoki CrN umożliwiła swobodne poruszanie się ziaren ścierniwa SiC między dwoma ciałami, inicjując formę zużycia przez toczenie (*three-body abrasive wear*). Przy trzykrotnie większym obciążeniu dystans między dwoma ciałami zmniejszył się, tym samym uniemożliwiając swobodne poruszanie się cząstek ścierniwa w węźle tarcia, co zainicjowało powstanie formy zużycia przez bruzdowanie (*two-body abrasive wear*).